

Numerical analyses for the dimensioning of fiber reinforced precast concrete lining segments for ram thrust forces

Paolo Cucino
SWS Engineering S.p.A.

Dimitri Rizzardi
SWS Engineering S.p.A.

Luca Schiavinato
SWS Engineering S.p.A.

Alberto Meda
University of Rome Tor Vergata

ABSTRACT

Fiber reinforcement is increasingly used in civil works to strengthen materials which otherwise possess a brittle failure mode. In mechanized tunneling, precast concrete lining design and reinforcement dimensioning is generally driven by ram forces during TBM advance and results in a considerable amount of localized reinforcement.

This paper describes the design of two sets of precast concrete lining of approximately 10m diameter which differ for segment geometry and number of rams. The paper highlights how the use of steel-fiber reinforcement to resist ram thrust forces, results in advantages and economies not restricted to TBM advance stage, *i.e.* easier production and assembly of the conventional reinforcement cage due to simpler geometry, and higher performance during handling and positioning.

INTRODUCTION

The mechanized excavation of tunnels is gradually evolving toward more versatile solutions. Evidences are the possibility of excavating larger tunnels and of facing different geological conditions (*e.g.* from soft soil to hard rock) with a single machine.

The liner usually installed at the back of the shielded machines (Tunnel Boring Machines or shields) is a ring of precast concrete. The circular shape guarantees a better static behavior than the sections adopted in conventional excavations. The ring is compressed and bending stresses are very limited. The installation consists in the sequential assembly of its constituent segments. To avoid the system to be labile, each segment is connected to the other ones of its same ring and of the previously installed ring. Once the ring is closed, a filler is grouted to ensure the confinement and to regularize the load application from the ground to the liner.

The design of the supporting system can be based on empirical or analytical formulations. Every loading condition experienced by the segment must be considered: from the formwork removal phase to the operating phase in the long term.

Focusing on the Tunnel Boring Machines, there are two commercial possibilities. The first is to use a TBM realized *ex novo*. The second is to use a reconditioned machine sets according to the current requirements. Also formworks and parts of the prefabrication plant are usually recycled in couple with a reconditioned TBM. This second case is the one examined in this paper. It means that the typology of the TBM is already defined and only minor changes can be implemented:

- the typology of the segment is defined according to the typology of the available machine and formworks;
- it is possible to define in detail the design procedure of the precast segments.

In this context, it has been tested the employment of steel-fiber reinforced elements. Fiber reinforced materials are living a fast pulse and development thanks to the new scientific and technologic achievements that allow:

- to develop approaches for the definition of their material properties;
- to verify the behavior at the large scale through physical models;
- to define the computation and test methodologies following the most recent national and international guidelines;
- to validate numerical modeling through non-linear analyses.

In this paper are presented the numerical analyses for the dimensioning of fiber reinforced precast concrete lining segments for ram thrust forces. These forces generally have high values, because they must overcome the friction and crack the rock at the contour of the shield.

In the following sections it is highlighted the necessity of representing the real geometry of the segment and of the advancement system of the machine to reach sufficiently reliable values of radial and circumferential traction stresses.

It is important to point out the influence of circumferential stresses generated by thrust jacks. Some designers consider them negligible because of the confinement given by the adjacent segments of the ring. This paper shows (in accordance with several international guidelines) the relevance of these stresses in the definition of the stress field of each precast segment. In the design phase, the information obtained by these analyses should contribute to the definition of the features of the boring machine and of the resistant model capable of absorbing those stresses.

CHARACTERISTICS OF THE FIBER REINFORCED CONCRETE

The fiber reinforced concrete (FRC) adopted it is classified according to the Model Code 2010. Considering the similarities of the compression behavior of the FRC and of the concrete matrix without fibers, the reference for the compressive properties is the DM 08. The resistance class chosen for compression is the C50/60.

For the tensile behavior, the reference is the Model Code 2010, which recommend using the results of a three-point bending test (standard EN 15651). In order to identify the constitutive law of the material in the tensile condition, it is recalled the residual strength defined in EN 14651:

$$f_{R,j} = \frac{3 F_j l}{2 b h_{sp}^2}$$

where:

- $f_{R,j}$ [N/mm²] is the residual bending strength at the opening of a crack CMOD = CMOD_j with $j = 1, 2, 3, 4$.
- F_i [kN] is the load measured at a CMOD = CMOD_j with $j = 1, 2, 3, 4$, (Figure 1);
- l [mm] is the distance between the supports;
- b [mm] is the specimen width;
- h_{sp} [mm] is the distance between the apex of the notch and the top of the specimen.

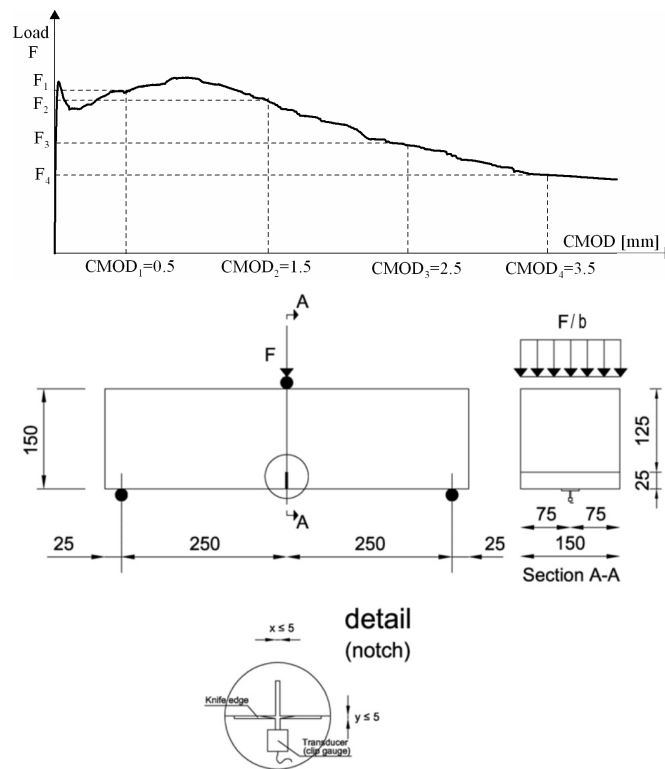


Figure 1. Tensile characterization of fiber reinforced concrete (EN 14651, MC2010)

In accordance with Model Code 2010, a rigid plastic constitutive equation, based on the strength values defined above, is adopted.

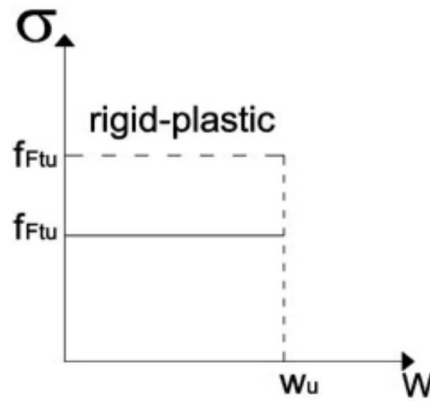


Figure 2. Rigid-plastic tensile constitutive equation

The reference value of the tensile strength is given by:

$$f_{FTu} = \frac{f_{R3}}{3}$$

In order to classify the FRC according to Model Code 2010, it is necessary to refer to two parameters: f_{R1k} and f_{R3k} . The FRC class adopted is 4.0 C. This results in a concrete characterised by a characteristic strength f_{R1k} higher than 4.0 MPa and the ratio between f_{R1k} and f_{R3k} in the range $0.9 \leq f_{R3k}/f_{R1k} \leq 1.1$. Consequently, the characteristic strength f_{R3k} will be higher than 3.6 MPa.

Table 1. Parameters of the FRC adopted

Compressive strength class	C50/60
Characteristic compressive cubic strength of concrete at 28 days	$R_{ck} = 60$ MPa
Characteristic compressive cylinder strength of concrete at 28 days	$f_{ck} = 50$ MPa
Partial factor for concrete	$\gamma_c = 1.5$
Design value of concrete compressive strength (long term)	$f_{cd} = 33.33$ MPa
Design value of concrete compressive strength (short term)	$f_{cd} = 28.33$ MPa
Characteristic residual strength of FRC for CMOD = 0.5 mm	$f_{R1k} = 4.0$ MPa
Characteristic residual strength of FRC for CMOD = 2.5 mm (C50/60)	$f_{R3k} = 3.6$ MPa
Characteristic residual strength of FRC for CMOD = 2.5 mm (C12/15)	$f_{R3k} = 2.0$ MPa
Tensile ultimate residual strength for the rigid-plastic model (C50/60)	$f_{Ftuk} = 1.2$ MPa
Partial safety factor for the tensile strength of FRC	$\gamma_F = 1.5$
Design value of tensile post-cracking strength (C50/60)	$f_{Ftud} = 0.8$ MPa

The fiber typology applied is DRAMIX 4D 80/60 BG. Tests conducted by the producer show that this product has a resistance $f_{R1k} = 4.0$ MPa, thanks to the high tensile resistance, ductility and anchoring capacity values of steel fibers. The ductility and the anchoring capacity are targeted to be effective on $0.1 \div 0.3$ mm cracks. The result is a durable and watertight structure. The 4D series is also the ideal solution for combining steel fibers and other reinforcement methods.

Table 2. Features of DRAMIX 4D 80/60 BG fibers

Length	60 mm
Diameter	0.75 mm
Aspect ratio (l/d)	80
Minimum tensile strength	> 1800 MPa
Ultimate elongation	< 4%

The stress-strain relation, at the Ultimate Limit State, for the fiber reinforced material is defined according to paragraph 5.6.5 of the Model Code 2010.

With a mesh size of the elements of the numerical model equal to 4cm, the tensile resistance law is assumed as follows in Table 3 and Figure 4.

Looking at the compressive strength, the material is considered linear elastic until the resistance limit equal to f_{cd} at 0.35%.

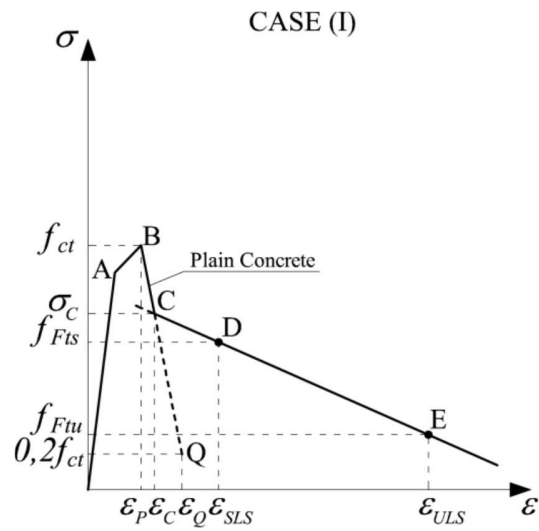


Figure 3. Stress-strain relations at SLS for softening behavior of FRC (MC2010-fig.5.6-11)

Table 3. Tensile stress-strain relation for fiber reinforced segments

ε [-]	σ_t [MPa]
0.000000	0.00
0.000067	2.57
0.000150	2.85
0.000507	2.21

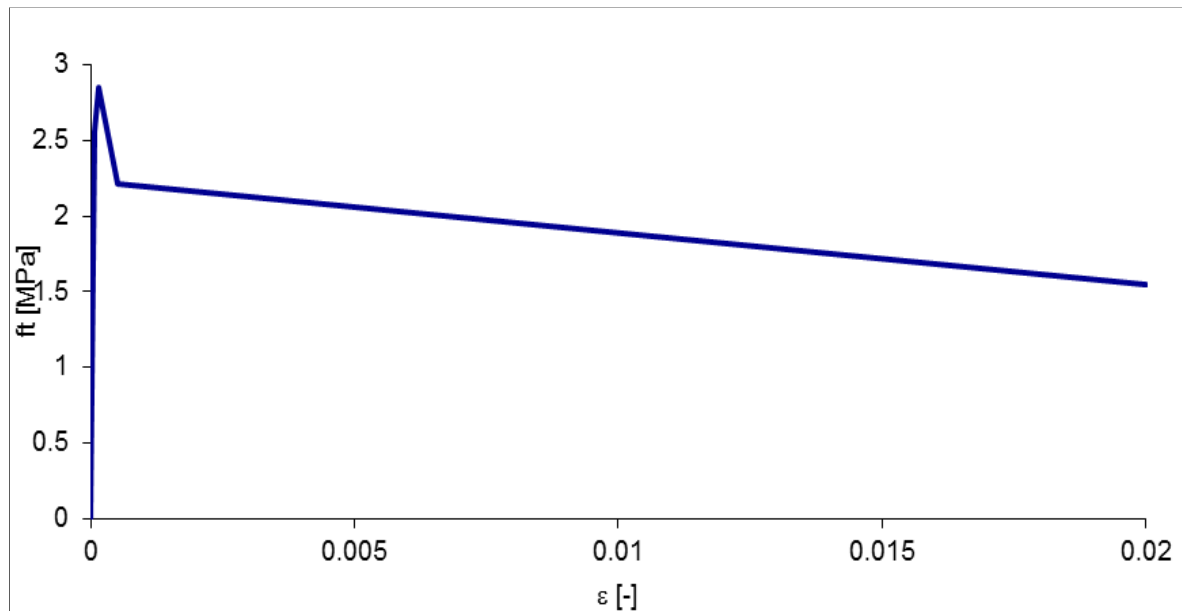


Figure 4. Tensile stress-strain relation for fiber reinforced segments

CASE STUDIES

Machine and Lining ring typology

The characteristics of the two examined cases are reported in this subsection.

Case 1. The tunnel is realized with a shielded Dual Mode TBM. This machine is studied to cope with both stone and non-cohesive material, allowing the excavation in the mutable geotechnical and geomechanical conditions along the track. The characteristics of the coating ring installed are:

- internal diameter 9.60m
- element thickness 0.35m
- ring typology 8+0 elements (big key)
- number of thrust groups 24 groups of two jacks each (three groups per segment).

The exact scheme is shown in Figure 5. Considering a traditional reinforcement, the necessary steel quantities are shown in Figure 6.

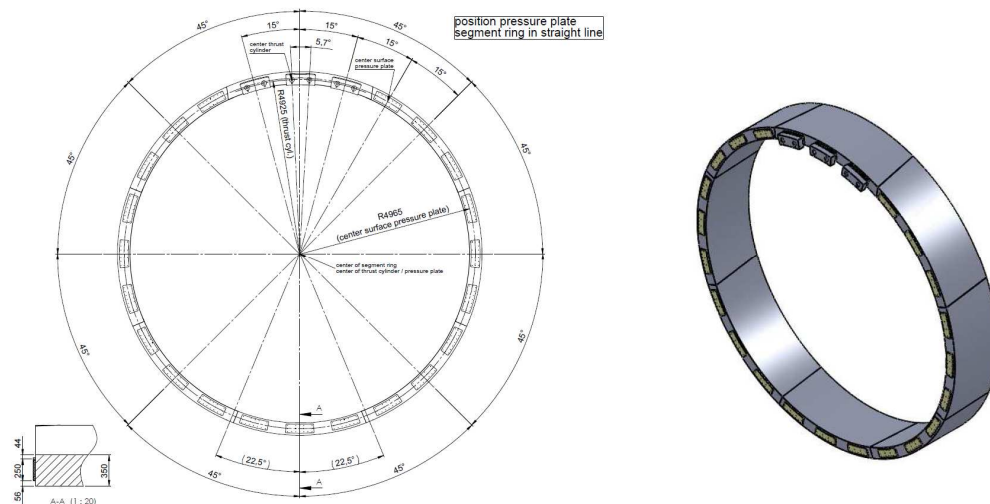


Figure 5. Scheme of the precast segments liner of Case 1

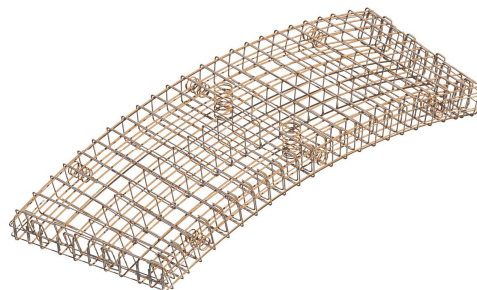


Figure 6. Reinforcement for the standard segment of Case 1

Case 2. The tunnel is realized with a shielded EPB TBM. This machine is studied to cope with both rock masses and non-cohesive material under the water table, allowing the excavation in the mutable geotechnical and geomechanical conditions along the track. The characteristics of the coating ring installed are:

- internal diameter 9.60m
- element thickness 0.32m
- ring typology 6+1 elements (big key)
- number of thrust groups 13 groups of three jacks each (two groups per segment).

The exact scheme is shown in Figure 7.

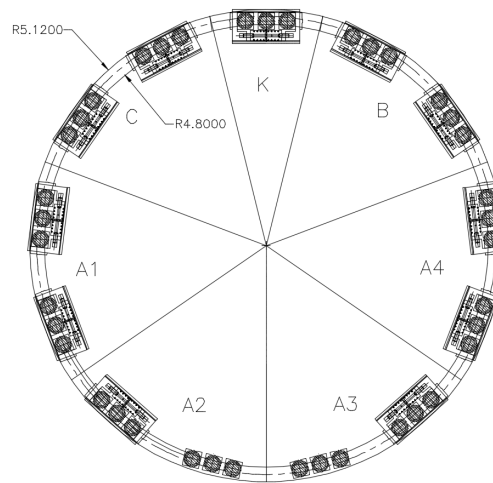


Figure 7. Scheme of the precast segments liner of Case 2

The design condition defines a maximum thrust force (exceptional condition) of 102,000 kN. Considering a traditional reinforcement, the necessary steel quantities are shown in Figure 8.



Figure 8. Reinforcement for the standard segment of Case 2

Numerical models in presence of diffused reinforcement

Description of the model methodology. A solid non linear model, realized and computed using the ABAQUS code, is considered for the analyses. The 3D geometry of the segment is generated with the extrusion of the transversal section. The surface is subdivided and sectioned in order to identify the zones loaded by the jacks and to differentiate the boundary conditions. The decomposition of the geometry into subregions is a preliminary condition to obtain a regular and consistent mesh of the model, an essential requirement for achieving reliable results.

To simulate the confinement given by the adjacent segments, their extremities appear in the model, as highlighted in Figure 9. These support elements allow modeling a hard contact interaction at the interface. Two different typologies of cinematic boundary condition are applied:

1. hard contact interaction which simulates the confinement given by the other segments of the current ring;
2. elastic springs which simulate the confinement given by the segment of the previous ring.

The hard contact is preferred to other boundary restrains for its effectiveness in simulating the normal and tangential interactions at the interface. In the normal direction, it allows the mutual compression, without interpenetration, of the element. In case of mutual traction, adhesion forces are not provided and the detachment occurs. In the tangential direction, no restrains are considered. The detachment generated by ram forces is allowed, avoiding the creation of spurious tractions, which would significantly distort the results. Friction forces, which increase the confinement and therefore the resistance of the concrete, are conservatively neglected.

The elastic springs, simulating the confinement given by the previous ring, are preferred to non linear spring because of the only-compressive stress state they are subjected to. A non linear behavior would have been unjustifiably too onerous in terms of computation.

The importance of the density and regularity of the mesh has already been pointed out. For the segment, finite solid C3D8R elements (8-node linear brick, reduced integration, hourglass control) with maximum dimension of $40 \times 40 \times 40 \text{ mm}^3$ are adopted. For the lateral supports a denser mesh of the same C3D8R elements is adopted, to achieve a higher precision in these contact zones. The maximum dimension of the elements is $25 \times 25 \times 25 \text{ mm}^3$.

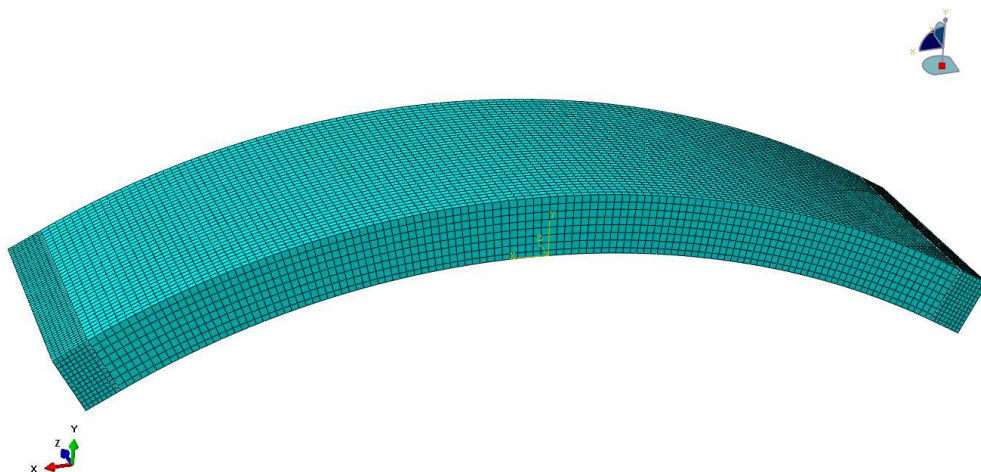


Figure 9. Finite solid element mesh for the model

Interaction between the constituting elements of the model

As already pointed out, the interaction between the constituting elements of the F.E.M. 3D model are described by the following formulations:

- **Hard contact:** defines the contact interaction between the adjacent segments.
Many engineering problems involve contact between two or more components. In these problems a force normal to the contacting surfaces acts on the two bodies when they touch each other. If there is friction between the surfaces, shear forces may be created that resist the tangential motion (sliding) of the bodies. The general aim of contact simulations is to identify the areas on the surfaces that are in contact and to calculate the contact pressures generated. In a finite element analysis contact conditions are a special class of discontinuous constraint, allowing forces to be transmitted from one part of the model to another. The constraint is discontinuous because it is applied only when the two surfaces are in contact. When the two surfaces separate, no constraint is applied. The analysis has to be able to detect when two surfaces are in contact and apply the contact constraints accordingly. Similarly, the analysis must be able to detect when two surfaces separate and remove the contact constraints. By default, contact pairs in Abaqus/Standard use a pure master-slave contact algorithm: nodes on one surface (the slave) cannot penetrate the segments that make up the other surface (the master), as shown in Figure 10. The algorithm places no restrictions on the master surface; it can penetrate the slave surface between slave nodes. Due to the strict master-slave formulation, you must be careful to select the slave and master surfaces correctly in order to achieve the best possible contact simulation. Some simple rules to follow are:
 - the slave surface should be the more finely meshed surface;
 - if the mesh densities are similar, the slave surface should be the surface with the softer underlying material.

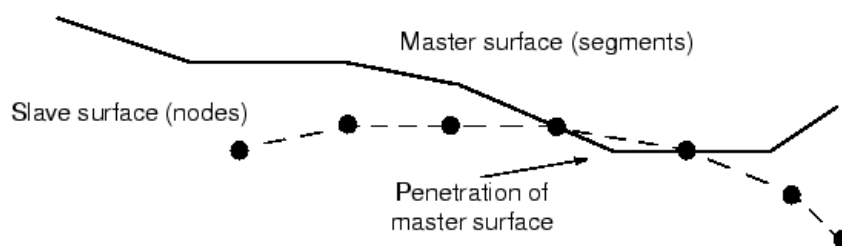


Figure 10. The master surface can penetrate the slave surface

- **Embedded:** allows the perfect adherence between the concrete and the reinforcement. The embedded element technique is used to specify that an element or group of elements is embedded in “host” elements. For example, the embedded element technique can be used to model rebar reinforcement. Abaqus searches for the geometric relationships between nodes of the embedded elements and the host elements. If a node of an embedded element lies within a host element, the translational degrees of freedom at the node are eliminated and the node becomes an “embedded node.” The translational degrees of freedom of the embedded node are constrained to the interpolated values of the corresponding degrees of freedom of the host

element. Embedded elements are allowed to have rotational degrees of freedom, but these rotations are not constrained by the embedding. Multiple embedded element definitions are allowed.

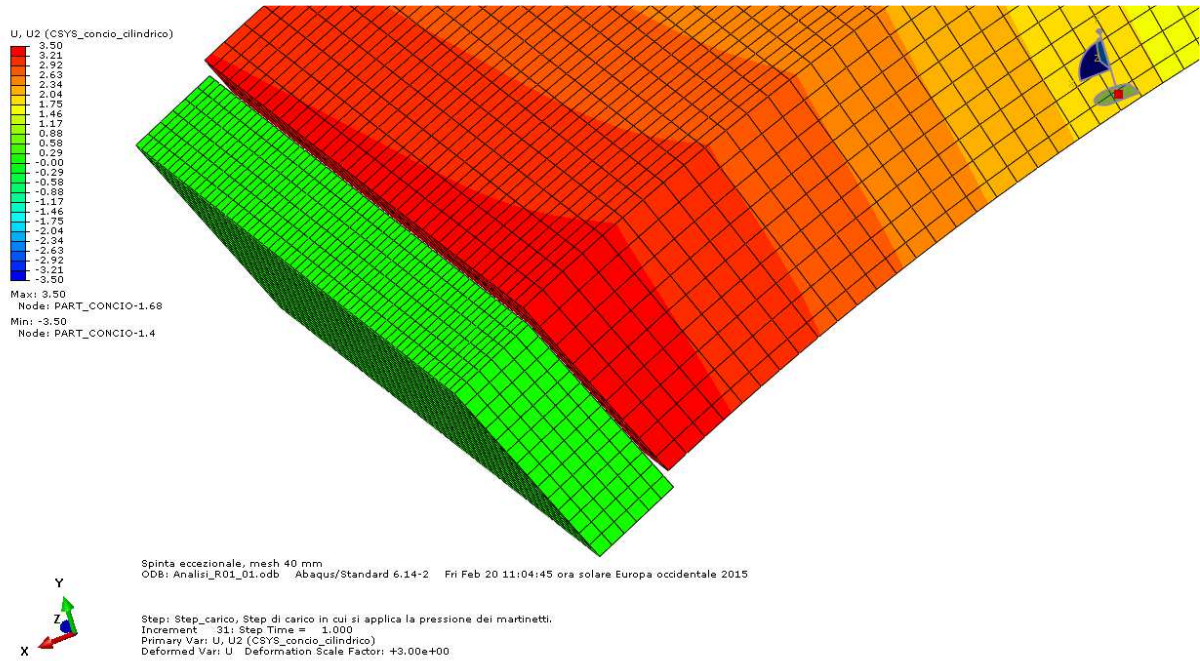


Figure 11. Detail showing the detachment allowed by the contact elements

The design condition defines a maximum thrust force (exceptional condition) of 100,000 kN, for both the analyzed cases.

Case 1. The acting load is given by the total thrust force times the number of jacks (2) of every group pushing the segment (3 groups) over the total number of jacks (48). The result is a ram force of 21,500 kN on the points of application.

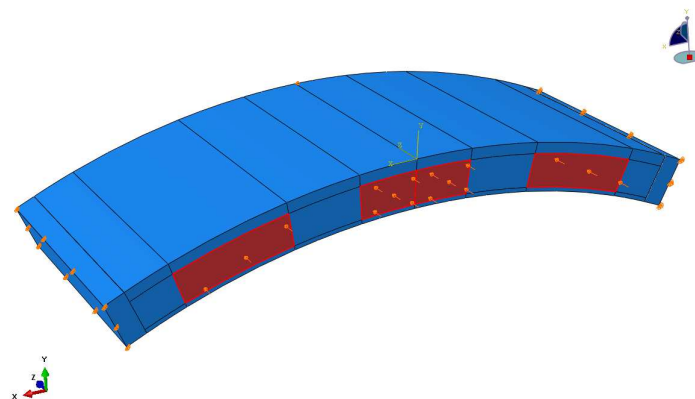


Figure 12. Loading scheme of the element, Case 1

For a better understanding of the functioning of the system, the loading has been incremented up to the instability condition. The results of the computation converge until a maximum ram force of 122,500 kN (22.5%).

Figure 13-Figure 16 present the stresses for Case 1. Considering the theoretical load condition, the maximum circumferential traction is registered in the portion between the contact plates. These tense zones are rather superficial. Below the plates, stresses do not exceed the tensile peak resistance of the material, which remain in the elastic field. Similar stress values are reached in the lateral zones.

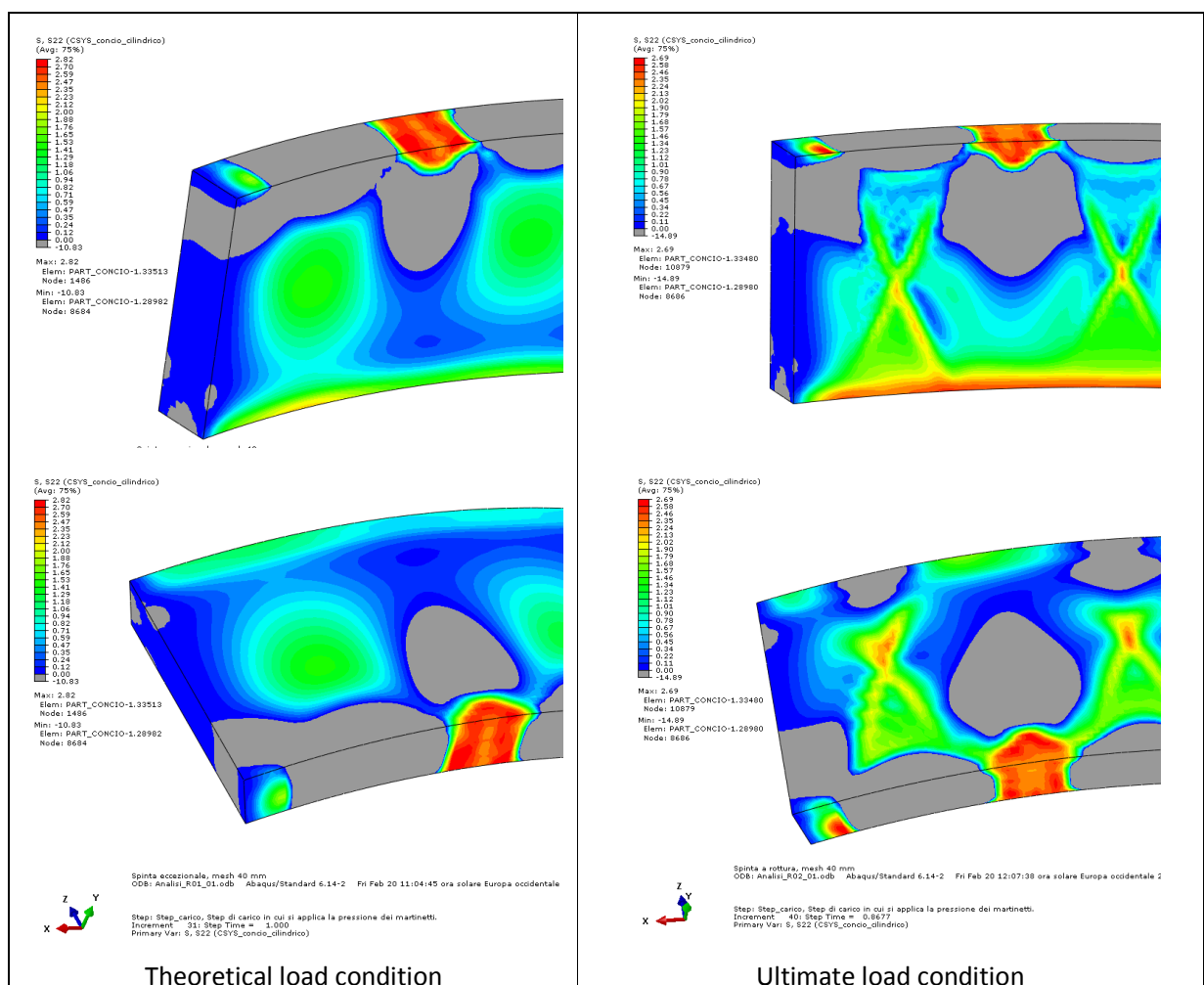


Figure 13. Comparison between circumferential traction in standard and ultimate conditions, Case 1

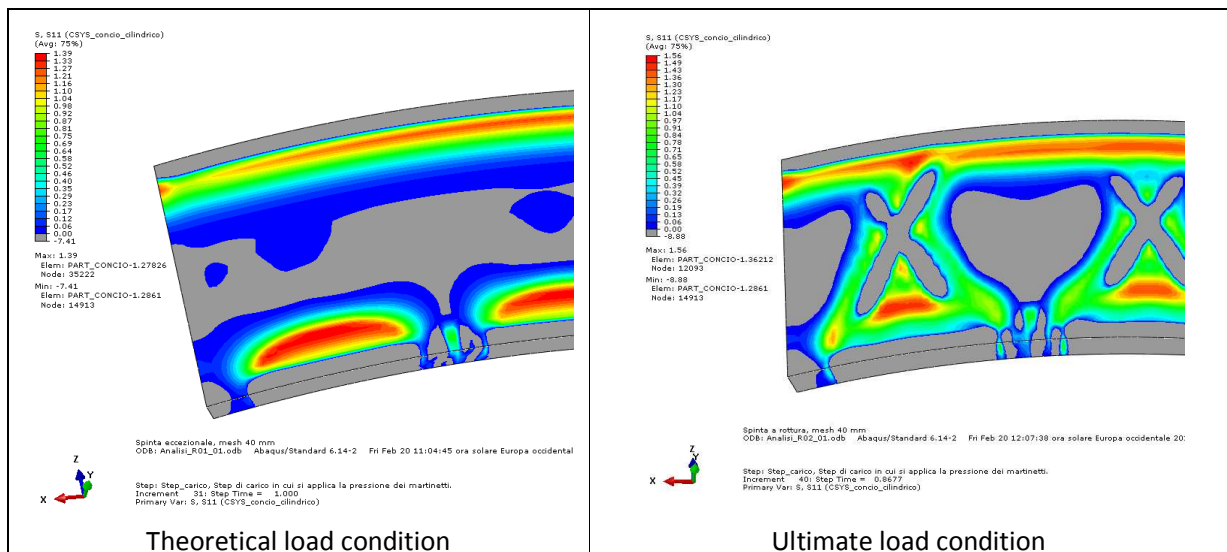


Figure 14. Comparison between radial traction in standard and ultimate conditions, Case 1

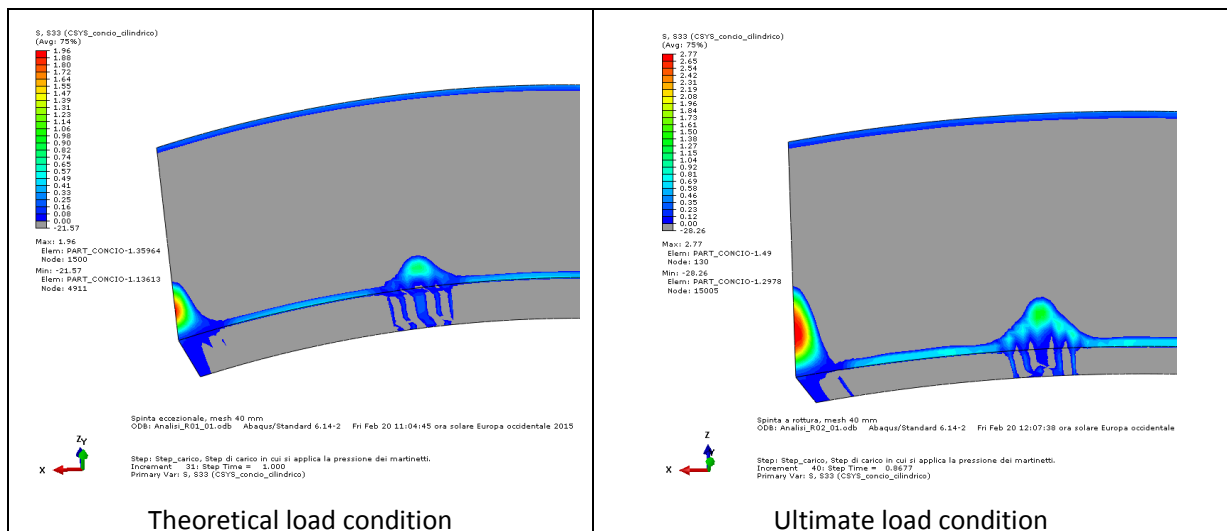


Figure 15. Comparison between longitudinal traction in standard and ultimate conditions, Case 1

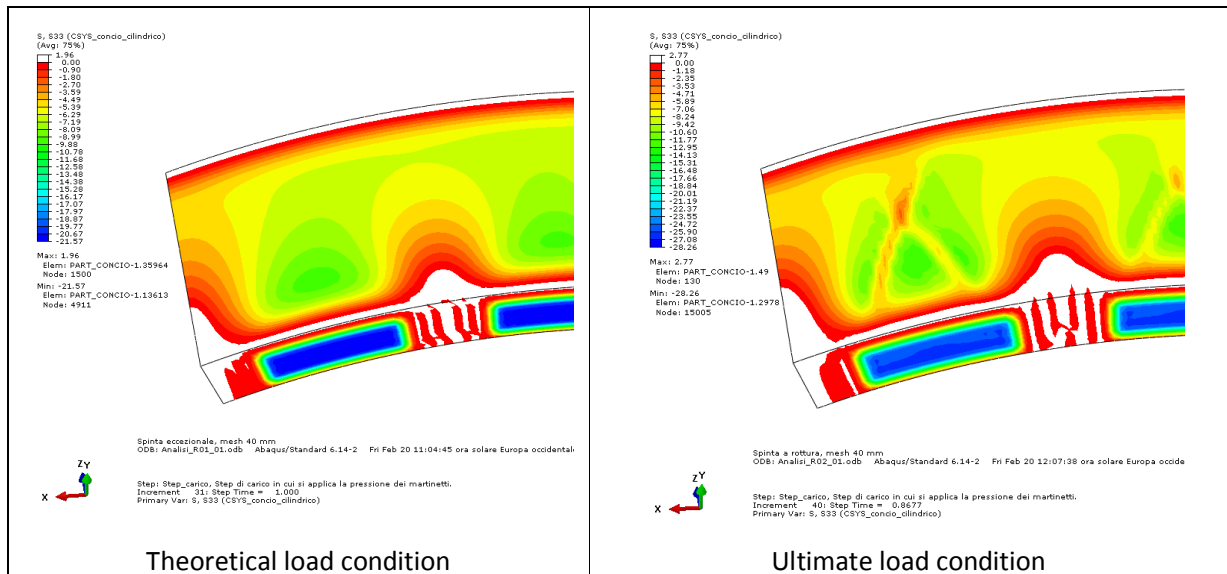


Figure 16. Comparison between longitudinal compression in standard and ultimate conditions, Case 1

Case2. The acting load is given by the total thrust force times the number of jacks (3) of every group pushing the segment (2 groups) over the total number of jacks (39). The result is a ram force of 25,200 kN on the points of application.

The computation does not reach the convergence. The stability is achieved for a loading equal to the 85% of the design one.

Two possible solutions are analyzed:

- increase the size of the loading plates;
- adoption of a mixed reinforcement system.

The first solution implies an enlargement of about 50cm (25cm per side) of the loading zones, consequently the tense zones are reduced. The cost of this solution is a limitation of the operability of the machine.

The second solution is evaluated the more effective, also considering the slenderness of the segment. The results obtained for the mixed reinforcement system are presented in the next subsection.

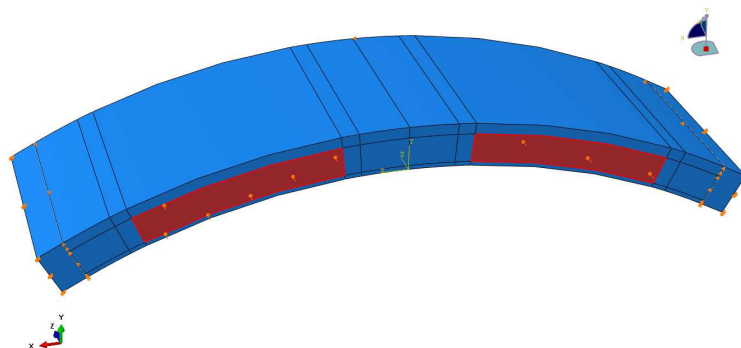


Figure 17. Loading scheme of the element, Case 2

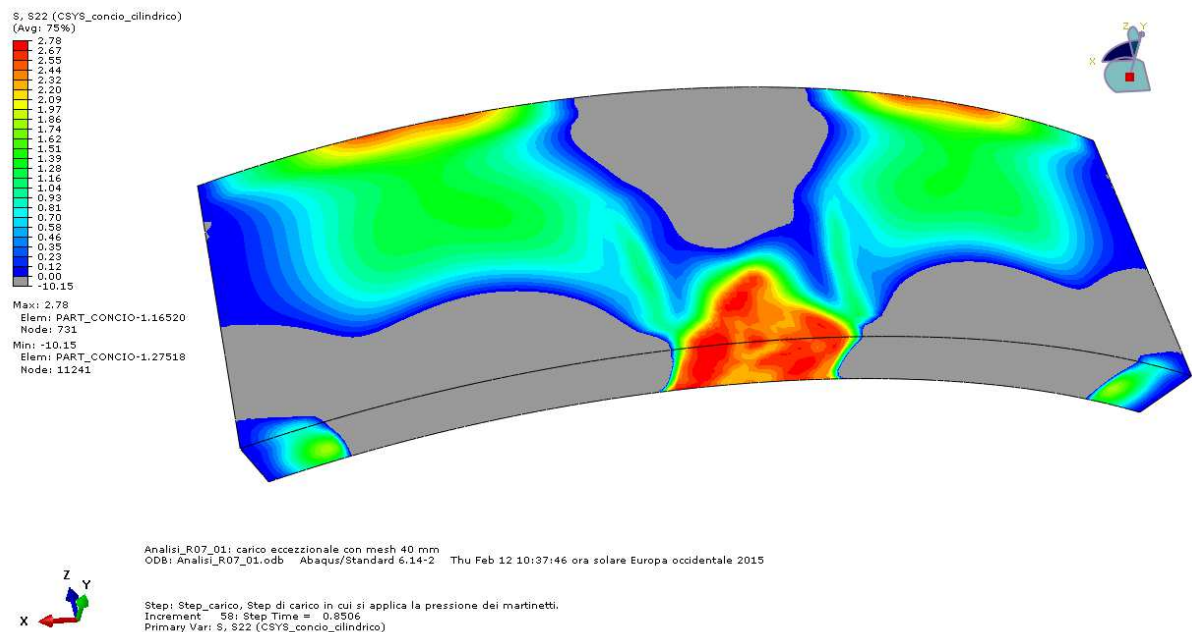


Figure 18. Circumferential traction in the ultimate condition at the 85% of the theoretical load, Case 2

Numerical model of mixed reinforcement system (Case 2)

The reinforcement in question, are modelled using axial load resisting elements (truss) “embedded” in the solid element mesh. The nodes of the monodimensional elements are merged with the nodes of the tridimensional ones, ensuring the congruence of the displacements and strains.

The analysis show a significant improvement in the behavior of the segment, which can now support the application of the entire design load.

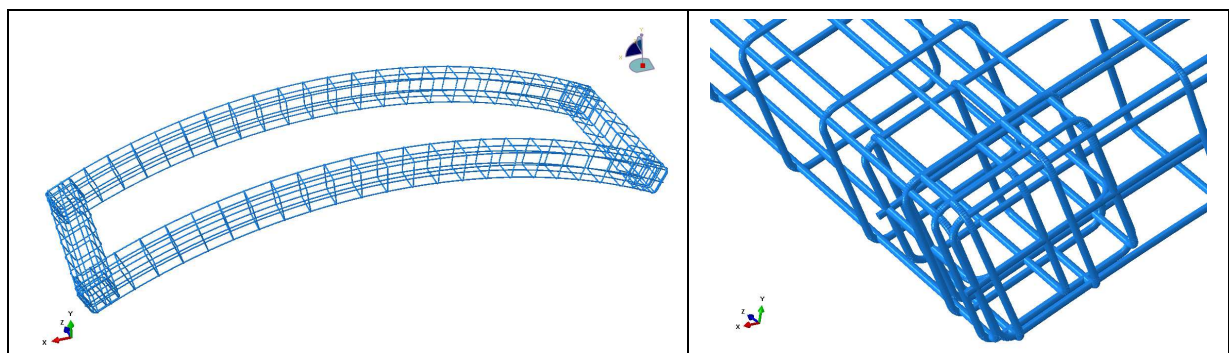


Figure 19. Geometry of the monodimensional element composing the reinforcement

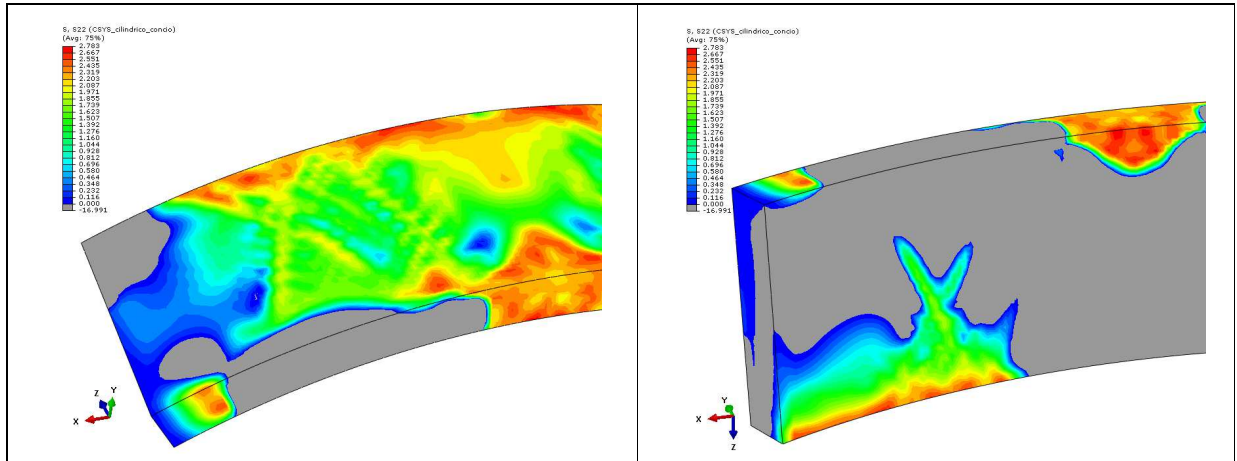


Figure 20. Circumferential traction at the intrados and extrados in standard condition, Case 2

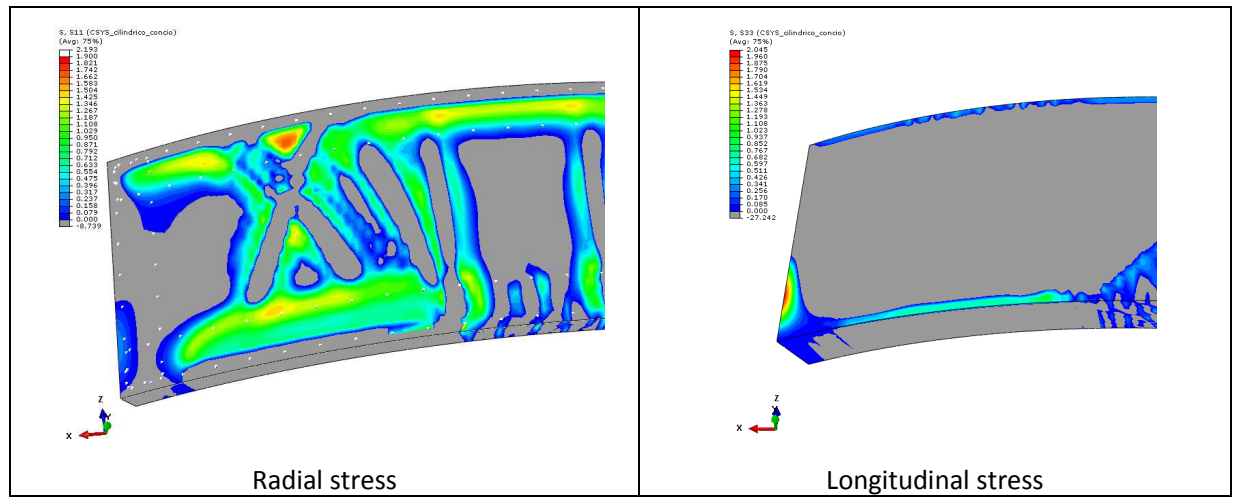


Figure 21. Radial and longitudinal traction in standard condition, Case 2

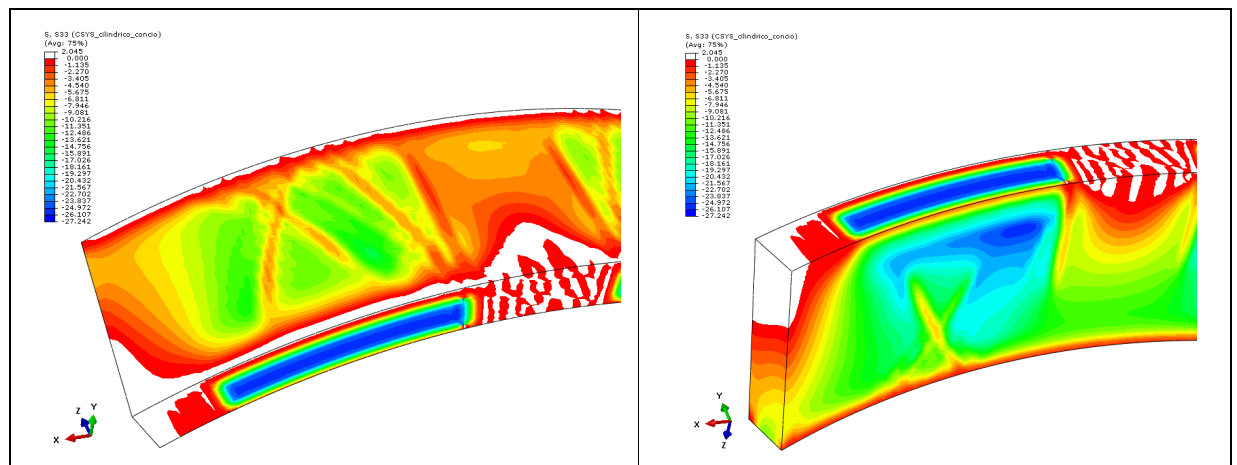


Figure 22. Longitudinal compression at the intrados and extrados in standard condition, Case 2

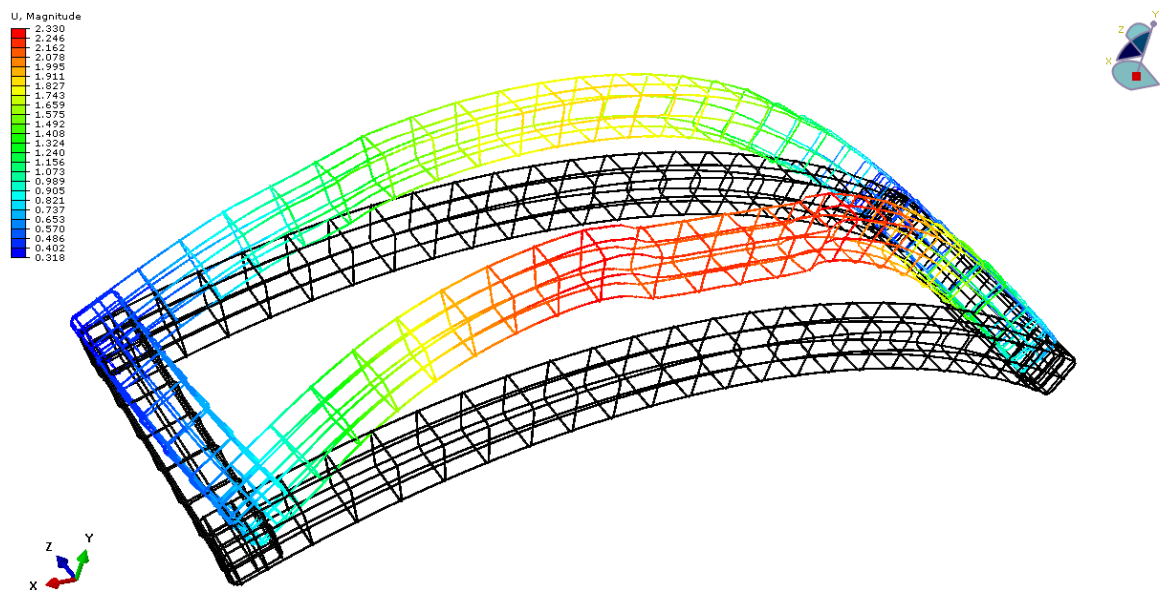


Figure 23. Deformation of the reinforcement system [mm]

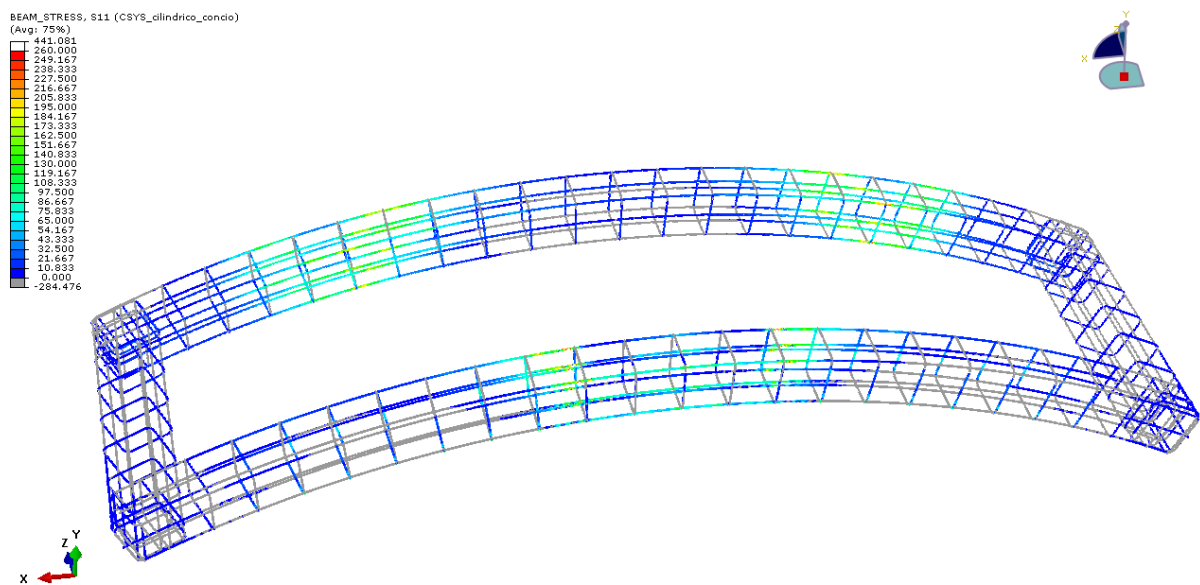


Figure 24. Circumferential traction in the ultimate condition at the 85% of the theoretical load, Case 2

CONCLUSIONS AND REMARKS

In this paper, different typologies of supporting segments are compared. The aim is to evaluate the possibility of simplifying the prefabrication procedures acting a complete, or partial, substitution of the traditional reinforcement with diffused steel fibers.

Two cases, with a similar geometry and thrust systems, are analyzed. Their comparison is based on the circumferential stresses, which are the most critical and influence the structural dimensioning.

In the first case the segment is pushed by 3 thrust groups. Results show a gradual increase of the stresses and of the material exploitation. In this condition it is verified the possibility of completely replace the traditional reinforcement with the diffused one.

In the second case only 2 thrust groups for each segment are employed. The numerical simulation generates unstable results, due to the failure which occurs in the central zone of the segment. With the addition of perimetric reinforcement, the fiber reinforced material is effectively exploited, in similarity to case 1, and the segment is verified. Even if such perimeteric reinforcement is not taken into account in the structural bending checks, it is important to consider it for the local analysis of contact zones.

The structures are dimensioned according to the aspects and the checks required for the form stripping, the transport, the storage, the installation and the exercise phases. The adoption of steel fibers guarantees significant advantages during all of these phases. Examples reported in literature show a relevant improvement in the resistance to point loads and chipping, which are frequently induced during mechanized excavations and can affect the durability of the structure.